Available online at www.sciencedirect.com

SCIENCE DIRECT

Journal of Crystal Growth 267 (2004) 47–59

JOURNAL OF CRYSTAL GROWTH

www.elsevier.com/locate/jcrysgro

Effect of growth kinetics on the structural and optical properties of quantum dot ensembles

V.G. Dubrovskii[a], G.E. Cirlin[b], Yu.G. Musikhin[a], Yu.B. Samsonenko[b], A.A. Tonkikh[a,*], N.K. Polyakov[b], V.A. Egorov[b], A.F. Tsatsul'nikov[a], N.A. Krizhanovskaya[a], V.M. Ustinov[a], P. Werner[c]

[a] *Ioffe Physical Technical Institute of the Russian Academy of Sciences, Politekhnicheskaya 26, 194021 St.-Petersburg, Russia*
[b] *Institute for Analytical Instrumentation of the Russian Academy of Sciences, Rizhsky pr.26, 190083 St.-Petersburg, Russia*
[c] *Max-Planck Institut für Mikrostrukturphysik, Weinberg 2, D-10620 Halle, Germany*

Received 17 February 2004; accepted 23 March 2004

Communicated by R. Kern

Abstract

The growth kinetics influence on the structural and optical properties of quantum dot ensembles in the Ge/Si(1 0 0) and InAs/GaAs(1 0 0) heteroepitaxial systems is studied theoretically and experimentally. A kinetic model of the stress-driven formation of quantum dots is developed providing a description of the time evolution of island size and density depending on the growth temperature, on the growth rate and on the total amount of deposited material. The quantum dot ensembles in the Ge/Si and InAs/GaAs systems are grown by molecular beam epitaxy at different conditions and studied by applying atomic force microscopy, transmission electron microscopy and photoluminescence spectroscopy. Theoretical and experimental results provide a detailed quantitative characterization of quantum dot ensembles in terms of their size and density depending on the technologically controlled growth conditions and provide a way for a kinetically controlled engineering of quantum dot ensembles with the desired properties.
© 2004 Elsevier B.V. All rights reserved.

PACS: 68.10.Jy; 68.55−a; 68.55.Jk; 81.15.−z

Keywords: A1.Kinetics; A3.Molecular beam epitaxy; A3.Quantum dots

1. Introduction

Concerning semiconductor materials, a continuously increasing interest from the viewpoints of fundamental physics and promising device applications has recently turned towards the quantum dot (QD) heterostructures [1]. Three-dimensional carrier confinement in QD leads to the dependence of the operating wavelength of QD-based optoelectronic devices on the average size of islands. The surface density of islands determines the intensity of luminescence. The major technological method to fabricate dense arrays of coherent strained

*Corresponding author. Physics of semiconductor, Heterostructures Laboratory Ioffe, Physico-Technical Institute, 194021 Politechnicheskaya 26, Saint-Petersburg, Russia; Tel.: +78122479350; fax: +78122479178.

E-mail address: alex234@newmail.ru (A.A. Tonkikh).

0022-0248/$ - see front matter © 2004 Elsevier B.V. All rights reserved.
doi:10.1016/j.jcrysgro.2004.03.055

islands is their direct formation during molecular beam epitaxy (MBE) and related growth techniques [1]. The technological need of a controlled production of QD heterostructures with desired properties stimulates the studies of the growth conditions influence on the structural and optical characteristics of QD ensembles.

If the material is deposited onto a substrate at a constant substrate temperature, growth rate and the exposition of structure upon the interruption of QD layer growth is performed at the same temperature, the major control parameters of the MBE growth in a particular heteroepitaxial system with given material constants are [2]: (i) the substrate temperature, (ii) the growth rate, (iii) the total amount of deposited material after the growth interruption and (iv) the exposition time before capping of the surface. In the case of III–V group nanostructures, the III/V fluxes ratio should be added to this list. Many experimental works have been concentrated on studying the influence of MBE growth conditions on the structural characteristics of QD ensembles in different heteroepitaxial systems. In particular, the experiments show an increase in the QD lateral size with a simultaneous decrease in their density when the substrate temperature is increased. In the case of so-called hut clusters in the Ge/Si(1 0 0) system, this effect has been described, for example, by Abstreiter et al. [3] and Yakimov et al. [4]. In the case of the InAs/GaAs(1 0 0) system, such a temperature dependence of QD ensemble has been demonstrated, for example, by Ledentsov et al. [5]. Several authors observed an increase in the density of QD at an increasing growth rate with a corresponding decrease in their size, both in the Ge/Si(1 0 0)[3] and InAs/GaAs(1 0 0) [6–8] systems. The lateral size of islands increases with the effective thickness, while the geometrical shape of islands undergoes a morphological transformation. In the Ge/Si(1 0 0) system, one observes a transition from a hut to a dome shape. The typical lateral size of hut clusters amounts to 15–20 nm [9] while the lateral size of domes ranges from 50 to 100 nm [10]. In the InAs/GaAs(1 0 0) system, the island shape remains approximately pyramidal when increasing the amount of deposited material, but their aspect ratio decreases [5,11]. It should be noted that in the majority of semiconductor heteroepitaxial systems, including the Ge/Si and InAs/GaAs, the Stranskii–Krastanow growth mode is dominant, i.e. the formation of islands occurs only after the effective thickness exceeds a certain critical value [1].

Concerning the theories of heteroepitaxial growth in the mismatched systems, a detailed description of island formation process is complicated by the coexistence of equilibrium and kinetic effects that are equally important in the island formation process. While the experimentally observed dependence of the QD size and density on the system energetics, on the lattice misfit, on the substrate temperature and on the effective thickness can be generally explained by various equilibrium models [12–14], the observed growth rate dependence of the QD structural parameters clearly indicates the role of kinetic effects. At the moment it is generally recognized that the QD formation is essentially stress-driven: the islands are formed because the elastic energy in the island is lower than in the wetting layer (WL) [1]. An important step forward was taken by Shchukin et al. [12], who found that within a certain range of material constants and lattice misfit, the combined effect of strain-induced renormalization of surface energy and elastic relaxation on island edges may result in a minimum of equilibrium free energy. This minimum relates to particular energetically favorable size and a narrow size distribution. Another equilibrium approach, which incorporates the growth of WL, coherent island formation and ripening was proposed by Daruka and Barabasi [13]. However, the further progress in theoretical understanding of the island formation mechanisms requires the development of a kinetic theory that can predict the time evolution of a QD array under essentially non-equilibrium conditions. An important contribution in this direction was made by Osipov et al. [15], who showed that the initial stage of coherent island formation during MBE growth can be well described within the frame of classical nucleation theory. Some of the present authors proposed a model that enables one not only prediction of the time evolution of the island size distribution and WL thickness but also allows to find analytically the dependences of

size and density of islands on the kinetic growth conditions valid for MBE [16]. Recent experiments [15] documented a considerable decrease in the WL thickness during the formation of islands. Because of that, theoretical models of Refs. [15,16] assume that the dominant mechanism of island growth is the stress-driven diffusion flux of surface atoms from the WL to the growing islands.

In this work we theoretically and experimentally investigate the structural and optical properties of QD ensembles in the Ge/Si(1 0 0) and InAs/GaAs(1 0 0) systems at the initial stage of heteroepitaxial growth. The study is restricted to the case of a diluted ensemble of small islands, when no interaction between islands is observed and no hut to dome transformation occurs. Special attention is paid to the investigation of the temperature and growth rate influence on the properties of QD ensembles. The theoretical description bases on the model given in Ref. [16], which allows a quantitative description of structural properties of QD ensemble depending on the MBE growth conditions. Growth experiments were carried out in different MBE machines at different growth rates, substrate temperatures, effective thickness and exposition times. The growth of QD layer was stopped at an effective thickness whose value is not far above the critical thickness relating to the onset of transformation from two-dimensional layer growth to three-dimensional islanding (2D–3D transformation) for the both systems studied. Additionally, in the InAs/GaAs(1 0 0) system, we have also studied the samples with subcritical effective thickness. The grown samples were analyzed applying transmission electron microscopy (TEM), atomic force microscopy (AFM) and photoluminescence (PL) techniques. The results of numerical simulations are compared to the experimental data obtained by different diagnostics. Our results are summarized in graphs presenting the island lateral size and density as functions of the substrate temperature and the growth rate. We will demonstrate that the QD arrays exhibit similar qualitative performance for the both heteroepitaxial systems studied. It will be shown that the predictions of kinetic model are in a good correlation with the experimental data, and that the structure of studied QD ensembles is mainly controlled by the MBE growth kinetics, not so strong by thermodynamics.

2. Theory

We consider that the material is deposited onto a substrate surface stabilized at temperature T with a growth rate V, which is constant at $t<t_0$ and zero at $t>t_0$. Herein, t_0 denotes the moment at which the growth of an island layer is interrupted. The time dependence of the total amount of deposited material H (effective thickness) is therefore given by $H(t)=Vt$ at $t<t_0$ and $H_0=Vt_0$ at $t>t_0$, where H_0 is the effective thickness of an island layer after the material flux is switched off. Here and below we measure thickness in the numbers of monolayers (ML). The Stranski-Krastanow growth is characterized by the existence of a flux-independent equilibrium WL of thickness h_{eq} found from the Müller–Kern criterion [17]. The equilibrium thickness of WL relates to the thermodynamic equilibrium in a heteroepitaxial system when the elastic energy of WL equals the wetting energy; the value of h_{eq} depends only on the system energetics and on the temperature. The formation of islands is possible only from a *metastable* WL with a thickness $h>h_{eq}$. Therefore, superstress $\zeta=h/h_{eq}-1$ is the measure of WL metastability [6,15,16].

Consider the system geometry in the Stranski–Krastanow growth mode shown schematically in Fig. 1. The islands are assumed as being the pyramids with square base $L\times L$ and contact angle

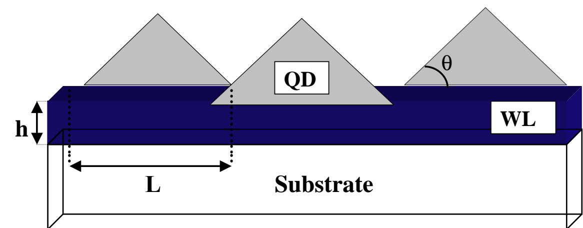

Fig. 1. Scheme on the system geometry of the Stranski–Krastanow growth mode: WL—wetting layer of thickness h, QD—quantum dot ensemble with average size L and surface density N, θ—contact angle.

θ, the aspect ratio $\beta = \tan\frac{\theta}{2}$. The model for the free energy of coherent island formation (in $k_B T$ units, k_B is Boltzmann constant) of Ref. [16] reads

$$F(i) = Ai^{2/3} - B\zeta i. \qquad (1)$$

Here i is the number of atoms in the island, the parameters A and B are given by

$$A \equiv \frac{[\sigma(\theta)/\cos\theta - \sigma(0)]}{k_B T}\alpha^2 l_0^2$$
$$B \equiv \ln\left(\frac{\Psi_0}{d_0(1-z)\lambda\varepsilon_0^2}\right)\frac{(1-z)\lambda\varepsilon_0^2 l_0^2 d_0}{k_B T}. \qquad (2)$$

The first term in Eq.(1) stands for an energetically unfavorable process of formation of additional surface area of island facets. The parameter A is the ratio of the difference in surface energy of the island and of the WL area covered by this island to the thermal energy, σ is the surface energy of the deposit (values $\sigma(0)$ and $\sigma(\theta)$ corresponds to the substrate surface plane and four equivalent pyramid facets) with the allowance for the strain-induced renormalization [1], l_0 is the average distance between atoms on the surface, d_0 is the height of a ML and $\alpha = (6d_0 \cot an\theta/l_0)^{1/3}$ is the geometrical factor. The second term in Eq.(1) is the difference in chemical potentials of atoms in the island and in the WL. The parameter B contains two factors: the logarithm of the ratio between the wetting energy on the deposit-substrate interface Ψ_0 [17] and the gain in elastic energy due to the 2D–3D transition (ε_0 relates to the lattice misfit, λ is the elastic modulus of the deposit, $z(\theta)$ is the relative relaxation of elastic stress in the island [18,19]) and the ratio between the elastic energy gain to the thermal energy. According to the Müller-Kern model [17], the wetting energy Ψ_0 is determined by the difference between the interface energies of the substrate surface (σ_s) and the sum of interface energy of deposit surface ($\sigma_d = \sigma(0)$) and the energy of interface between them (σ_{s-d}): $\Psi_0 = \sigma_s - \sigma_d - \sigma_{s-d}$.

From Eqs. (1) and (2) follows the expression for the nucleation barrier in $k_B T$ units:

$$F(\zeta) = \frac{4}{27}\frac{A^3}{B^2\zeta^2} \simeq \frac{T_e}{T\varsigma^2}. \qquad (3)$$

Eq. (3) shows that the activation barrier decreases with increasing the WL thickness (superstress) and the temperature, the last equality is valid for modest variations in T, when the material constant are approximately constant. The characteristic quasi-equilibrium temperature T_e contains all material constants of a given heteroepitaxial system, its lattice misfit parameter and the island shape in the form

$$T_e = \frac{4}{27k_B}\frac{[\sigma(\theta)/\cos\theta - \sigma(0)]^3(6\cot an\theta)^2}{[(1-Z(\theta))\lambda\varepsilon_0^2]^2\ln^2[\Psi_0/d_0(1-Z(\theta))\lambda\varepsilon_0^2]}. \qquad (4)$$

The temperature T_e determines the height of the nucleation barrier of coherent islands at given WL thickness; its value is independent on the kinetic parameters of MBE growth. Eq. (4) demonstrates that T_e strongly decreases with the increase in the lattice misfit (the major dependence is $T_e \sim 1/\varepsilon_0^4$) and also decreases with increasing the contact angle θ. Consequently, the critical thickness is lower for the systems with larger misfit and for higher islands, because the higher islands have lower elastic stress energy than flatter ones [20]. The dependence of the island formation energy on the number of atoms in the island at different WL thickness for the parameters of the Ge/Si(1 0 0) system [15] is shown in Fig. 2.

As follows from the detailed analysis of Ref. [16], if the effective thickness of deposited material exceeds a certain critical thickness H_c ($H_0 > H_c$), the maximum WL thickness $h_c \approx H_c$, and the maximum superstress is $\zeta_c = h_c/h_{eq} - 1$ The maximum of WL thickness at $h = h_c$ is reached at the moment when the arrival of atoms to the WL from a molecular beam is equalized by the consumption of atoms from the WL by the growing islands. After that moment, the WL thickness h decreases because the consumption of atoms from the WL by the growing islands dominates, while the effective thickness H increases until the growth process is stopped. The critical effective thickness relating to the 2D–3D transformation onset can be associated with the maximum WL thickness, because the amount of material in the islands at the moment of 2D–3D transition is negligibly

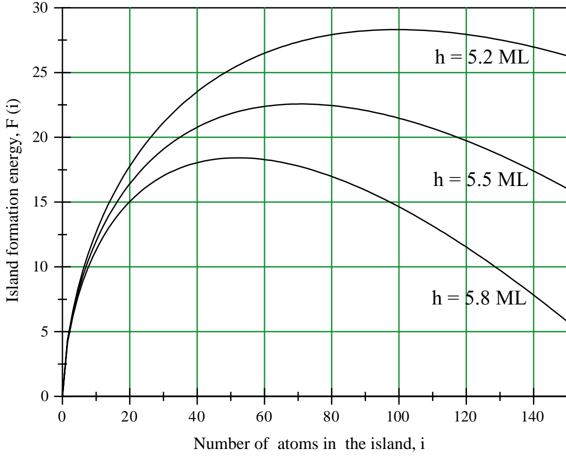

Fig. 2. Island formation energy for the parameters of the Ge/Si(1 0 0) system (λ= 1.27 × 10^{12} dyn/cm^2; $\varepsilon_0 = 0.042$, d_0= 0.145 nm, l_0= 0.395 nm, $\Psi_0 = 450$ erg/cm^2; $\sigma(0) = \sigma(\theta) = 800$ erg/cm^2, θ= 18°(z = 0.61) at T= 470°C and three different values of WL thickness.

small. At a maximum WL thickness, the nucleation rate of islands also reaches its maximum, therefore the islands nucleated at $h = h_c$ will remain the most representative in the island size distribution at a later stage of growth. The nucleation of islands is completed very soon after the WL thickness reaches its maximum. Implying the equation of material balance, the relationship between the critical thickness h_c and the kinetic parameters of the growth process is given by the self-consistent equation $F(\zeta_c) = \left(\frac{5}{2}\right)\ln Q$. Using Eq. (3), the expression for the critical thickness is found in the form

$$h_c \cong h_{eq}\left[1 + \left(\frac{2}{5}\frac{T_e}{T\ln Q}\right)^{1/2}\right]. \tag{5}$$

The kinetic control parameter Q introduced in Ref. [16] determines the time scaling of deposition and island formation processes [2] according to $Q = t_{eq}/\tau$, where $t_{eq} = h_{eq}/V$ is the time to grow the equilibrium WL on a bare substrate and τ is the average time interval between two consecutive attachments of atoms from WL to a growing island. As a ratio of characteristic times of macroscopic and microscopic processes, the parameter Q is very large (for typical conditions of MBE $Q > 100$). It is important that Q is reverse proportional to the growth rate and increases with the temperature approximately as the Arrhenius exponent:

$$Q \propto \frac{1}{VT}\exp\left(-\frac{T_D}{T}\right). \tag{6}$$

Here $T_D \equiv E_D/k_B$ is the characteristic diffusion temperature, E_D is the activation energy for the stress-driven diffusion of the surface atoms from the WL to the growing islands. The parameter Q decreases with the growth rate because the time to grow the flux-independent equilibrium WL at higher growth rate becomes shorter and increases with temperature because the diffusion processes proceed faster at higher temperatures and therefore the characteristic time of island growth shortens. Eq. (1) shows that despite the kinetic origin of critical thickness its numerical value is mainly determined by the surface energetics, the lattice misfit and the substrate temperature and only weakly depends on the growth kinetics, a conclusion which fits well with the experimental results [21] and with the conclusions of equilibrium models of heteroepitaxial growth [14]. The coefficient of proportionality in Eq. (6) at given h_{eq} and T_e can be easily found from Eq. (5), because the critical thickness h_c is controlled experimentally with high accuracy [1].

At the end of nucleation stage, the average size remains negligibly small during the whole stage of nucleation (i.e., of order of the critical size according to the classical nucleation theory), while the surface density of islands goes to the constant value. This value is found from the solution of evolution equation for the lateral size distribution of islands together with the equation of material balance on the substrate surface at the nucleation stage. The result of Ref. [16] is given by

$$N = \frac{4}{l_0^2}h_{eq}\frac{T}{T_e}\left(\frac{\ln Q}{Q}\right)^{3/2}. \tag{7}$$

A short-scale nucleation stage is followed by a considerably longer stage of the island size relaxation. At this stage, the island surface density established during the nucleation stage remains

approximately constant; the WL thickness decreases from its maximum to equilibrium value and the size L increases to its quasistationary value L_R. The described qualitative behavior of the QD array is valid as long as there is no considerable reduction in the island growth rate, which could be caused by the influence of strain-induced barriers for atom consumption (essential for large islands [19]) or by the so-called dipole–dipole elastic interaction of islands (essential at a high coverage of the surface [12]). After the size relaxation stage and the growth interruption, the effective thickness H equals H_0 and the WL thickness h goes to h_{eq}. The island density N equals its value established at the nucleation stage. The average size of islands L goes to its quasistationary value L_R [2,16]. The equation of material balance derived from the system geometry of Fig. 1 in this case reads

$$N\frac{L_R^3}{6}\tan\theta = (H_0 - h_{eq})d_0. \tag{8}$$

The right-hand side of this equation presents the total volume of islands per unit surface area. At the end of size relaxation stage all $H_0 - h_{eq}$ ML of deposited material should be distributed in the islands. The use of δ-shaped approximation for the island size distribution is approved because the distribution is approximately Gaussian and its width at the end of size relaxation stage is relatively small ($\Delta L_R/L_R \ll 1$). From Eqs. (4) and (5) follows the average size of islands at the end of size relaxation stage:

$$L_R = \left[\frac{3}{2}l_0^2 d_0\frac{(H_0 - h_{eq})T_e}{h_{eq}\quad T}\cot an\theta\right]^{1/3}\left(\frac{Q}{\ln Q}\right)^{1/2}. \tag{9}$$

Eqs. (7) and (9) together with Eq. (6) demonstrate that the surface density of islands decreases with an increasing substrate temperature and increases with the growth rate, while the average size of islands increases with the temperature and decreases with the growth rate [3–7] and that the structure of the QD ensemble is essentially kinetically controlled [16].

The time evolution of the average lateral size of islands L at the size relaxation stage [2] can be found in the form of reverse dependence $t(L)$:

$$\frac{t - t_c}{t_R} = \ln\left[\frac{(1 + l + l^2)^{1/2}}{1 - l}\right] - \sqrt{3}\arctan\left(\frac{2l + 1}{\sqrt{3}}\right) + \frac{\pi}{2\sqrt{3}} \equiv U(l). \tag{10}$$

Here, $l = L/L_R$, and t_R is the characteristic time of island size relaxation given by

$$t_R = \frac{0.47}{\ln^{1/3} Q}(t_c - t_{eq}). \tag{11}$$

Eqs. (10) and (11) are obtained from the solution of evolution equation for the average lateral size of islands at the size relaxation stage [16]. The time moments t_c and t_{eq} in Eqs. (10) and (11) are simply the times required to grow the WL of critical thickness h_c and of equilibrium thickness h_{eq}, respectively ($t_c = h_c/V, t_{eq} = h_{eq}/V$). The defined function $U(l)$ in the right-hand side of Eq. (10) contains no parameters of the model, therefore the dependence of relative average size l on the relative deposition time $(t - t_c)/t_R$ has a universal character shown in Fig. 3.

In principle, Eqs. (5)–(7) and (9)–(11) provide a complete description of the time evolution of QD ensemble at the size relaxation stage in terms of island average size and density. The main parameters of the model are the characteristic quasi-equilibrium temperature T_e and the diffusion temperature T_D. The value of T_e is determined by the energetic constants of a strained heteroepitaxial system and by

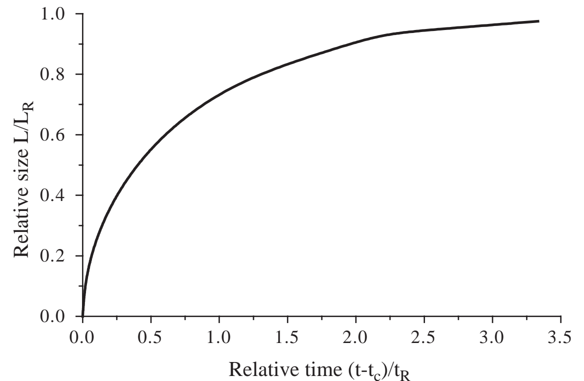

Fig. 3. Universal time dependence of relative lateral size at the size relaxation stage obtained from Eq. (10).

the geometrical shape of islands, while the value of T_D is determined by the mechanisms of stress-driven diffusion of atoms from the WL to the growing islands. To access the known effect of variation in the aspect ratio of islands [1,5], the contact angle θ could be adjusted to the experimentally measured values of aspect ratio, for example obtained by a cross-sectional TEM analysis. This relates to the case when the QD are more or less truncated pyramids. If the grown QD layer is cooled or capped immediately after the growth interruption, the time t in Eq. (10) relating to the observed lateral size is found simply as $t = H_0/V$, where H_0 is the effective thickness of a deposited QD layer. If the structure is exposed during a certain time interval Δt_{exp} before cooling or capping, $t = H_0/V + \Delta t_{exp}$. An exposition of structure therefore allows a more complete relaxation of the average size of islands, i.e. at the same growth conditions the islands are larger at longer exposition. The presented kinetic model provides a detailed characterization of QD ensemble depending on four control parameters of MBE growth, $N = N(T, V)$; $L = L(T, V, H_0, \Delta t_{exp})$. It is important that in the overcritical thickness range [2], the surface density depends only on the temperature and growth rate and does not change with further increase in the amount of deposit as well as with the exposition time, while the average size depends on the whole set of MBE growth conditions. It should be noted, however, that the model describes the kinetics of uncapped structures. Further relaxation of the system during the growth of cap layer may change the geometry of islands and even their size due to the diffusion exchange of atoms between the QD and the cap layer. When applying the model to the case of capped QD systems, we thus assume that these effects result in a minor change in the system geometry. Generalization of the model to include the kinetics of capped structures requires a separate study.

3. Experiment

3.1. Ge/Si(1 0 0) system

The temperature dependence of QD ensemble was investigated in the Ge/Si(1 0 0) heteroepitaxial system. Four samples of Ge islands on Si(1 0 0) surface were grown using Riber SIVA MBE machine. The substrate temperature T was fixed to 420°C, 450°C, 470°C and 500°C, respectively. The growth technique and characterization procedures are described in Ref. [22]. The growth rate of Ge was fixed to 0.035 ML/s for all samples. As the moment of growth interruption for each sample, an effective thickness of 6.2 ML of deposited Ge was chosen. The corresponding deposition time amounted to 180 s. Afterwards, the samples were studied by AFM using Digital Instruments Inc. setup.

A typical AFM image of Ge/Si(1 0 0) QD ensemble at a growth temperature T of 450°C is presented in Fig. 4. It was found the islands have a pyramidal shape with a square base. At higher substrate temperatures, the QD ensemble contains square and rectangular base islands. Rectangular islands are elongated in [1 0 0] direction, the L_x/L_y ratio ranges from 1.74 to 2.64 depending on the temperature. For all samples, the fraction of square base remains predominant. The aspect ratio of square base and elongated QD increases with increasing the substrate temperature. For square base islands, the variation in aspect ratio ranges from $\beta = 0.1$ at $T = 420$°C to $\beta = 0.24$ at $T = 500$°C. The average lateral size at 6.2 ML considerably increases with increasing the

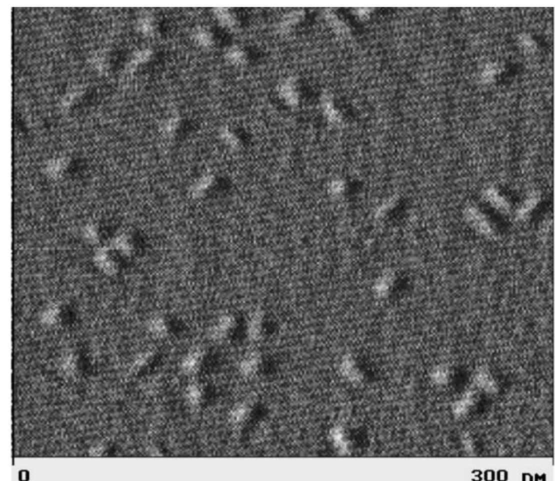

Fig. 4. AFM image of Ge/Si(1 0 0) QD at 6.2 ML, grown at $T = 450$°C. The scanned area amounts to 300×300 nm.

substrate temperature both for square base and elongated islands.

3.2. InAs/GaAs(1 0 0) system

The growth rate and temperature behavior of the structural and optical properties of QD ensembles was studied in the InAs/GaAs(1 0 0) system. Growth experiments were carried out on an EP1203 solid source MBE machine on semi-insulating GaAs (1 0 0) substrates. The effective thickness of the InAs layer was fixed to 2.0 ML for all samples. The InAs growth rate V was varied from 0.01 to 0.1 ML/s. Two series of samples were grown, for which the substrate temperature T during the deposition of the QD layer was kept at 440°C and 485°C, respectively. The As shutter was opened through the whole growth run. For each sample, the InAs QD layer was covered by a low-temperature GaAs cap immediately after the In deposition (i.e. with zero exposition). The active region was confined by two short-period superlattices of $GaAs/Al_{0.3}Ga_{0.7}As$ (25Å/25Å, 10 pairs) in order to prevent the carrier escape from the active region into the substrate and surface areas. These superlattices and the GaAs buffer layer were grown at 600°C. PL measurements were carried out in a standard lock-in configuration. The excitation was provided by a 514.5 nm Ar^+ laser. TEM measurements were carried out applying a Philips EM420 electron microscope. Typical TEM plan-view images of 2 ML InAs QD ensembles at different temperatures are shown in Figs. 5 and 6. Concerning the used diffraction contrast technique, the QD have a square base with sides parallel to the crystallographic $\langle 1\,1\,0 \rangle$ directions.

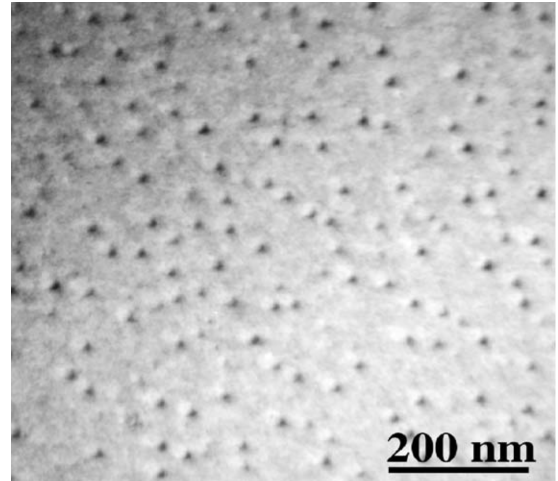

Fig. 5. TEM image of 2 ML InAs QD on GaAs(1 0 0) surface, T= 485°C, V= 0.03 ML/s.

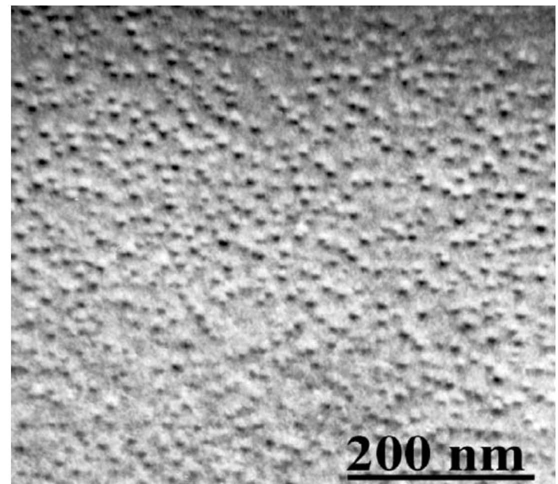

Fig. 6. TEM image of 2 ML InAs QD on GaAs(1 0 0) surface, T= 440°C, V= 0.05 ML/s.

As pointed out in Section 2, the theory predicts a possibility for the formation of coherent islands in subcritical thickness range, when the effective thickness is larger than the equilibrium WL thickness but lower than the critical thickness relating to the 2D–3D transition under the material flux. In this case, the formation of islands proceeds much slower than in overcritical thickness range. Also, at the same temperatures and growth rates the islands will be considerably larger in size and lower in density as compared to overcritical islands. To investigate the morphology and optical properties of subcritical structures, two series of InAs/GaAs(1 0 0) structures were grown, where the effective thickness of the InAs layer was fixed to 1.5 and 1.6 ML, respectively. The growth temperature was varied from 420°C to 485°C within both series.

The InAs growth rate was fixed to 0.03 ML/s for all samples. After the deposition of the InAs layer, the surface was exposed under the As_4 flux, the exposition time was varied from 1.5 to 2.5 min for

different samples. The active region was confined by two short-period superlattices of GaAs/$Al_{0.25}$-$Ga_{0.75}As$ (25Å/25Å, 5 pairs), grown at 585°C. The surface structure was controlled in situ by reflection high-energy electron diffraction (RHEED) system composed of a high sensitivity video camera, a videotape recorder and a computer. It has been found that during the deposition of InAs at $h_{tot} < 1.6$ ML the RHEED patterns remain streaky. The exposition of samples under the As_4 flux after switching off the source of In leads to the transition of RHEED patterns from streaky to spotty for all samples except the 1.5 ML sample grown at 485°C (for this sample, the formation of islands was not observed even at 90 s exposition). The moment of this transition is interpreted as the beginning of island nucleation. Further exposition of samples leads to the appearance of additional RHEED patterns corresponding to the diffraction from the island facet planes, the moment of their appearance can be associated with reaching the quasi-stationary size of islands. The optical properties of subcritical QD ensembles were subsequently studied by PL.

4. Results and discussion

4.1. Ge/Si(1 0 0) system

For a quantitative comparison of theoretical and experimentally measured temperature dependence of the average lateral size and the surface density of QD in the Ge/Si(1 0 0) system, calculations were made for the following model parameters of the Ge/Si(1 0 0) system: $\lambda = 1 \cdot 27 \times 10^{12}$ dyn/cm^2; $\varepsilon_0 = 0.042$, $d_0 = 0.145$ nm, $l_0 = 0.395$ nm, $\Psi_0 = 450$ erg/cm^2; $\sigma(0) = \sigma(\theta) = 800$ erg/cm^2 [15]. The diffusion temperature was fixed to $T_D = 7750$ K. Only the predominant fraction of square base islands was taken into consideration. The values of contact angle θ were varied to adjust the experimentally measured values of aspect ratio of Ge/Si nanoislands obtained from the cross-sectional analysis (column 2 in Table 1). The θ-dependent characteristic temperature T_e was calculated by means of Eq. (4), the relative relaxation of elastic stress in the island $Z(\theta)$ was found from the Ratsch–Zangwill approximation [18] and the equilibrium WL thickness h_{eq} was obtained using the Müller–Kern formula [16,17] (h_{eq} was found to be approximately 3.3 ML). The kinetic control parameter Q at different temperatures was calculated by means of Eq.(6) and the critical thickness by Eq. (5). The surface density of islands N was then found from Eq. (7) and the average lateral size $L(t)$ from Eqs. (9)–(11). The time t was related to 6.2 ML of deposited Ge at given growth rate V. Theoretical characteristics of the kinetics of QD formation and the structural parameters of 6.2 ML Ge/Si(1 0 0) QD ensembles at different growth temperatures are summarized in Table 1. The calculations show that the theoretical values of critical thickness =4.8–5.2 ML for the whole interval of substrate temperatures studied, which is in agreement with the experiment [3,4]. The surface density is predicted to decrease gradually from 5.7×10^{10} cm^{-2} to 1.7×10^{10} cm^{-2} as the temperature increases from 420°C to 500°C, while the lateral size of QD increases with temperature from 12 to 21 nm.The lateral size $L(t)$ is considerably smaller than the quasistationary size L_R because the interruption of growth at 6.2 ML with an immediate cooling of the surface does not allow a complete relaxation at the size relaxation stage.

Table 1
Theoretical characteristics of 6.2 ML Ge/Si(1 0 0) QD ensembles at different growth temperatures

T, (°C)	θ (deg)	h_c (ML)	N (10^{10} cm^{-2})	$L(t)$ (nm)	L_R (nm)
420	13	4.8	5.7	11.7	25
450	19	5.0	4.0	17.5	26
470	19	5.0	3.3	19.6	28
500	26	5.2	1.7	21.3	31

The comparison between the results of calculations and the AFM data for the temperature dependence of the average size and density of 6.2 ML Ge/Si QD ensembles is shown in Figs. 7 and 8. It is seen that theoretical and experimental curves are in a fairly good agreement with each other, the discrepancy at 470°C for the surface density and at 450°C for the average size could be associated with the existence of a fraction of elongated islands as well as with a space

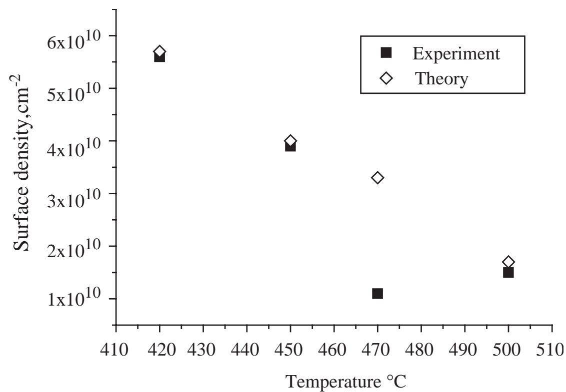

Fig. 7. Theoretical and experimental dependence of the surface density of 6.2 ML QD in the Ge/Si(1 0 0) system.

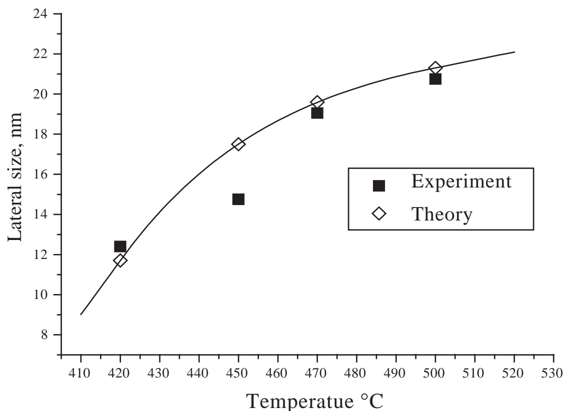

Fig. 8. Theoretical and experimental dependence of the average lateral size of 6.2 ML QD in the Ge/Si(1 0 0) system.

inhomogeneity of QD ensemble. Nevertheless, both dependences demonstrate the increase in lateral size of 6.2 ML Ge/Si QD from $L\approx 12$ to $L\approx 20$ nm with the corresponding decrease in their density from $N\approx 5.5\times 10^{10}$ to $N\approx 1.5\times 10^{10}\,\mathrm{cm}^{-2}$ at increasing the temperature from 420°C to 500°C, the effect which has been previously observed experimentally [3].

4.2. InAs/GaAs(1 0 0) system

The measured dependence of the PL peak position on the InAs growth rate at different substrate temperatures is presented in Fig. 9. A typical PL spectrum is shown in the inset in Fig. 9.

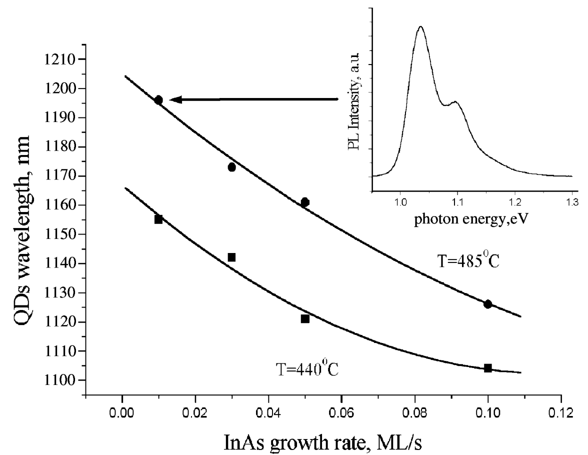

Fig. 9. Room temperature PL peak position from 2 ML InAs/GaAs(1 0 0) QD depending on the InAs growth rate at two different temperatures. Room temperature PL spectrum shown in the inset relates to the sample pointed by the arrow.

The two PL peaks are associated with the QD ground and excited states, respectively. Fig. 9 demonstrates that the PL peak position is gradually shifted towards a shorter wavelength range with increasing the growth rate for both series of different substrate temperature applied. At the same growth rate of InAs, the PL peak is always higher at 485°C than at 440°C. Therefore, the characteristic size of islands increases with an increasing of the growth temperature and a decreasing of the growth rate. The behavior of optical properties of InAs QD ensembles follows the general tendencies imposed by the kinetic limitations on the QD formation process [5–7] and is in qualitative agreement with the predictions of theoretical model presented in Section 2.

In order to make a quantitative comparison of the results of our TEM investigations of samples grown at different conditions with the predictions of the theoretical model, the calculations were performed for the following model parameters for a InAs/GaAs(1 0 0) system: $d_0 = 0.303$ nm, $l_0 = 0.429$ nm, $\alpha = 1.82\approx\mathrm{const}$ and $H_0 = 2$ ML. The value of T_D was fixed to 4700 K, the value of T_e was varied taking into account that $h_{eq}\approx 1$ ML and $h_{\tilde{n}}\approx 1.7-1.8$ ML (directly experimentally measured value [1]). The growth rate of InAs was varied from 0.01 to 0.1 ML/s for the two

Table 2
Theoretical characteristics of 2 ML InAs/GaAs(1 0 0) QD ensembles grown at different temperatures and growth rates

V (ML/s)	T (°C)	T_e (K)	h_c (ML)	N ($10^{10}\,cm^{-2}$)	L(t) (nm)	L_R (nm)
0.01	440	4630	1.70	2.8	16.3	18.5
0.03	440	7630	1.75	4.8	12.7	15.9
0.05	440	9900	1.77	6.7	11.0	14.7
0.1	440	11400	1.80	13	8.8	12.1
0.01	485	4590	1.68	0.62	23.1	27.0
0.03	485	8110	1.74	1.3	18.9	23.9
0.05	485	11300	1.77	1.7	17.1	20.2
0.1	485	13700	1.79	3.3	12.7	17.6

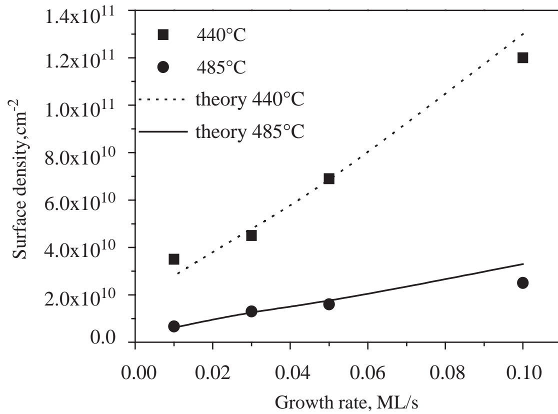

Fig. 10. Comparison of TEM data and the results of calculations for the density of 2 ML InAs QD on GaAs(1 0 0) surface grown at different growth rates and substrate temperatures.

chosen substrate temperatures of $T = 440°\tilde{N}$ and of $T = 485°\tilde{N}$, respectively. The results of simulations for the main characteristics of QD ensemble are presented in Table 2, where $L(t)$ is the average lateral size of InAs QD at 2 ML of deposited InAs. Theoretical and experimental dependences of QD size and density on the InAs growth rate at the two different growth temperatures are shown in Figs. 10 and 11, which quantitatively demonstrate the effect of the increase in the density with the simultaneous decrease in the size at high growth rates and low growth temperatures (the effect reported previously in Ref. [6,7]).

Concerning the characteristic exposition times required for the beginning of island formation and

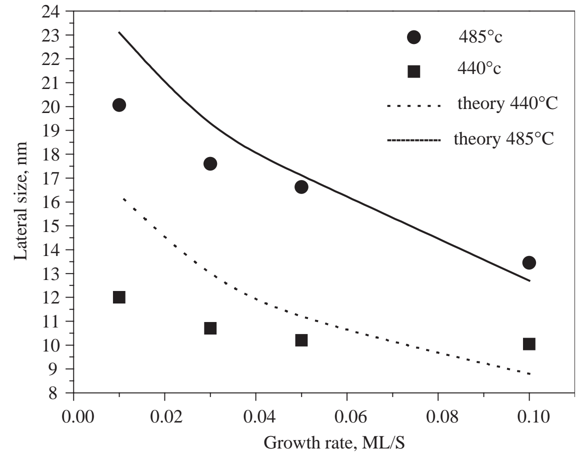

Fig. 11. Comparison of TEM data and the results of calculations for the average lateral size of 2 ML InAs QD on GaAs(1 0 0) surface grown at different growth rates and substrate temperatures.

the position of PL peaks from the subcritical InAs QD, our results are summarized in Table 3. The temperature dependence of the characteristic times of QD formation for 1.5 and 1.6 ML structures is presented in Fig. 12. These results demonstrate that the QD formation in 1.5 ML structures requires a longer exposition than in 1.6 ML due to a lower level superstress. The influence of growth temperature on the PL spectra of relaxed 1.6 ML QD ensembles is shown in Fig. 13. It is seen that the increase in the temperature leads to the shift of PL peak position towards a longer wavelength, i.e. the size of islands increases similarly to the overcritical QD structures.

5. Conclusions

We have investigated theoretically and experimentally the structural and optical properties of QD ensembles in the Ge/Si(1 0 0) and InAs/GaAs(1 0 0) system as functions of the growth temperature, growth rate, effective thickness and exposition time (in the case of subcritical InAs/GaAs structures). It is shown that there exists a good correlation between the results of simulations within the frame of the developed kinetic model and the experimental data obtained by AFM,

Table 3
Kinetics and optical characteristics of subsritical InAs/GaAs(1 0 0) structures

Sample	Effective thickness of InAs layer (ML)	Substrate temperature (°C)	Exposition time required for the QD formation (s)	QD PL peak position (eV)
A	1.6	485	13	1.079
B	1.6	450	4	1.117
C	1.6	420	2	1.169
D	1.5	485	> 90	—
E	1.5	450	20	1.130
F	1.5	420	15	1.140

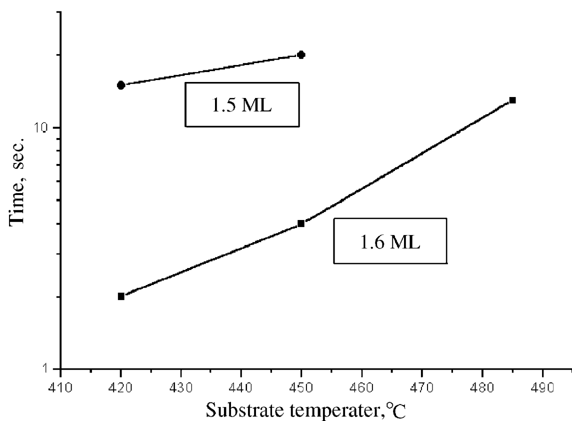

Fig. 12. Temperature dependence of characteristic times of QD formation in 1.5 and 1.6 ML InAs/GaAs(1 0 0) structures.

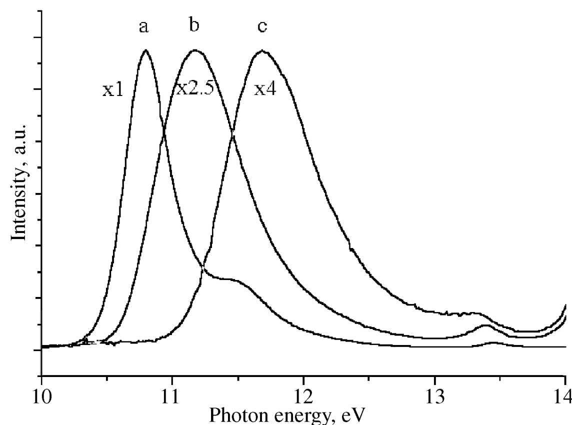

Fig. 13. Temperature dependence of PL spectra from 1.6 ML InAs/GaAs(1 0 0) QD for (a) $T = 485°C$, (b) $T = 450°C$ and (c) $T = 420°C$.

TEM and PL diagnostics of the grown structures for the both heteroepitaxial systems. It is found that the structural and optical properties of QD ensembles are essentially kinetically controlled. In particular, the QD density increases and their size decreases at higher growth rate and lower substrate temperature. In the 2 ML InAs/GaAs(1 0 0) system, the QD density reaches $1.2 \times 10^{11}\,cm^{-2}$ at $T = 440°C$ and $V = 0.1$ ML/s, and therefore could be used as the first layer of a vertically stacked QD structure to fabricate a very dense array with larger size of QD in the upper layers. It is important that the obtained results provide a quantitative characterization of QD ensembles in terms of their size and density depending on the technologically controlled growth conditions of MBE. This gives a possibility for a kinetically controlled engineering of QD ensembles with the desired properties for various applications.

Acknowledgements

The authors would like to thank U. Gösele for supporting the research in this subject, G.Gerth and A.Frommfeld for experimental help. V.G.D. wishes to thank S.A.Kukushkin and A.V.Osipov for helpful discussions of theoretical model. G.E.C. is grateful to the Alexander von Humboldt Foundation. The authors are grateful to the financial support obtained from different scientific programs of the Russian Ministry of Industry, Science and Technology and from the research grant of St.-Petersburg Scientific Center of the Russian Academy of Sciences.

References

[1] D. Bimberg, M. Grundmann, N.N. Ledentsov, Quantum dot heterostructures, Wiley, New York, 1999.

[2] V.G. Dubrovskii, Phys. Stat. Sol. (b) (2003), 238, R1.

[3] G. Abstreiter, P. Schittenhelm, C. Engel, E. Silveria, A. Zrenner, D. Meertens, W. Jäger, Semicond. Sci. Technol. 11 (1996) 1521.

[4] A.I. Yakimov, A.V. Dvurechenskii, Yu.Yu. Proskuryakov, A.I. Nikiforov, O.P. Pchelyakov, S.A. Teys, A.K. Gutakovskii, Appl. Phys. Lett. 75 (1999) 1413.

[5] N.N. Ledentsov, V.A. Shchukin, D. Bimberg, V.M. Ustinov, N.A. Cherkashin, Yu.G. Musikhin, B.V. Volovik, G.E. Cirlin, Zh.I. Alferov, Semicond. Sci. Technol. 16 (2001) 502.

[6] S. Kiravittaya, Y. Nakamura, O.G. Schmidt, Physica E 13 (2002) 224.

[7] R. Songmuang, S. Kiravittaya, M. Sawadsaringkam, S. Panyakeow, O.G. Schmidt, J. Crystal Growth 251 (2003) 166.

[8] P.B. Joyce, T.J. Krzyzewski, G.R. Bell, T.S. Jones, S. Malik, D. Childs, R. Murray, Phys. Rev. B 62 (2000) 10891.

[9] Y.-W. Mo, D.E. Savage, B.S. Swartzentruber, M.G. Lagally, Phys. Rev. Lett. 65 (1990) 1020.

[10] J.A. Floro, E. Chanson, L.B. Freund, R.D. Twesten, R.Q. Hwang, G.A. Lucadamo, Phys. Rev. B 59 (1999) 1990.

[11] M. Califano, P. Harrison, Phys. Rev. B 61 (2000) 10959.

[12] V.A. Shchukin, N.N. Ledentsov, P.S. Kop'ev, D. Bimberg, Phys. Rev. Lett. 75 (1995) 2968.

[13] I. Daruka, A.-L. Barabasi, Phys. Rev. Lett. 79 (1997) 3708.

[14] J. Tersoff, Phys. Rev. B 43 (1991) 9377.

[15] A.V. Osipov, F. Schmitt, S.A. Kukushkin, P. Hess, Appl. Surf. Sci. 188 (2002) 156.

[16] V.G. Dubrovskii, G.E. Cirlin, V.M. Ustinov, Phys. Rev. B 68 (2003) 075409.

[17] P. Müller, R. Kern, Appl. Surf. Sci. 102 (1996) 6.

[18] C. Ratsch, A. Zangwill, Surf. Sci. 293 (1993) 123.

[19] A.V. Osipov, S.A. Kukushkin, F. Schmitt, P. Hess, Phys. Rev. B 64 (2001) 205421.

[20] V.A. Shchukin, D. Bimberg, Rev. Mod. Phys. 71 (1999) 1125.

[21] J.-M. Gerard, in: Confined Electrons and Photons, E. Burstein, C. Weisbuch, (Eds.), Plenum Press, New York, 1995.

[22] G.E. Cirlin, V.A. Egorov, L.V. Sokolov, P. Werner, Semiconductors 36 (2002) 1294.